

# AutoCAT: Reinforcement Learning for Automated Exploration of Cache-Timing Attacks

Mulong Luo<sup>\*¶</sup>, Wenjie Xiong<sup>†‡¶</sup>, Geunbae Lee<sup>†</sup>, Yueying Li<sup>\*</sup>, Xiaomeng Yang<sup>‡</sup>,  
Amy Zhang<sup>‡§</sup>, Yuandong Tian<sup>‡</sup>, Hsien-Hsin S. Lee<sup>‡</sup>, and G. Edward Suh<sup>\*‡</sup>

<sup>\*</sup>Cornell University <sup>†</sup>Virginia Tech <sup>§</sup>UC Berkeley <sup>‡</sup>Meta AI

{ml2558,y13469}@cornell.edu, {wenjiex,geunbae}@vt.edu, {yangxm,amyzhang,yuandong,leehs,edsuh}@fb.com

<sup>¶</sup>Equal contributions.

**Abstract**—The aggressive performance optimizations in modern microprocessors can result in security vulnerabilities. For example, the timing-based attacks in processor caches are shown to be successful in stealing secret keys or causing privilege escalation. So far, finding cache-timing vulnerabilities is mostly performed by human experts, which is inefficient and laborious. There is a need for automatic tools that can explore vulnerabilities because unreported vulnerabilities leave the systems at risk.

In this paper, we propose *AutoCAT*, an automated exploration framework that finds cache timing-channel attack sequences using reinforcement learning (RL). Specifically, *AutoCAT* formulates the cache timing-channel attack as a guessing game between the attacker program and the victim program holding a secret, which can thus be solved via modern deep RL techniques. *AutoCAT* can explore attacks in various cache configurations without knowing design details and under different attacker and victim configurations, and can also find attacks to bypass certain detection and defense mechanisms. In particular, *AutoCAT* discovered *StealthyStreamline*, a new attack that is able to bypass detection based on performance counters and has up to a 71% higher information leakage rate than the state-of-the-art LRU-based attacks on real processors. *AutoCAT* is the first of its kind using RL for crafting microarchitectural timing-channel attack sequences and can accelerate cache timing-channel exploration for secure microprocessor designs.

## I. INTRODUCTION

As we use computers to handle increasingly sensitive data and tasks, security has become one of the major design considerations for modern computer systems. For example, from the hardware perspective, microarchitecture-level timing channels have emerged as a major security concern as they allow leaking of information covertly with a high bit-rate and bypassing the traditional software isolation mechanisms. The timing-channel attacks are also shown to be an even more serious problem when combined with speculative execution capabilities [35], [42].

Unfortunately, developing a system that is sufficiently secure and efficient (high-performance) at the same time is quite challenging in large part because it is difficult to evaluate the security of a system design. By definition, a security vulnerability comes from an unknown bug or an unintended use of a system feature, which is difficult to know or quantify at design time. While formal methods and cryptography can provide mathematical guarantees, it is difficult to scale the formal proofs to complex systems and security

properties in practice. As a result, today’s security evaluation and analyses largely rely on human reviews and empirical studies based on known attacks or randomized tests. However, the security evaluation based on known attack sequences manually discovered by humans makes it difficult to assess the security of a new microarchitecture design or a defense mechanism. Vulnerabilities in new microarchitectures are often left unnoticed for a long time, and defense mechanisms are often found vulnerable to new attack sequences even when they are similar to the known ones. For example, while caches existed in microprocessors for a long time, Bernstein’s cache-timing attack was reported back in 2005 [6] followed by multiple variations such as evict+time (2006) [53], flush+reload (2014) [92], flush+flush (2016) [22], etc. New attacks in caches are still being reported recently, e.g., attacks in cache replacement states (2020) [9], [86], streamline (2021) [65], and attacks using cache dirty states (2022) [16].

This paper proposes to leverage reinforcement learning (RL) to automatically explore attack sequences for microarchitectural timing-channel vulnerabilities, and demonstrate the feasibility of this approach using cache timing channels as a concrete example. RL has been shown to achieve super-human performance in multiple competitive games (e.g., Go and Chess [70], DoTA 2 [5]) without starting from existing human knowledge. In this paper, we show that microarchitecture-level timing-channel attack can also be formulated as a *guessing game* for an attacker program, and is a good fit for RL. In this case, an RL agent can learn by self-playing the game many times in a well-defined environment, which is provided by real hardware or efficient simulation infrastructures commonly used for architecture studies. The experiments show that our RL framework, named *AutoCAT*, can automatically adapt to a variety of cache designs and countermeasures, and find cache-timing attacks, including known attack sequences and ones that are more efficient than known attack sequences.

While the use of machine learning (ML) for system security has been explored in the past, the previous work largely focused on performing or detecting *known attack sequences* on known system designs. For example, ML models with supervised learning are used in side-channel attacks to recover secrets [37], [44], [45], [83], [89], [93]. Similarly, ML models can be trained with known attack traces for intrusion detection [38]. This paper

asks a different question: can an RL agent automatically 1) learn system designs without explicit specifications and 2) generate attack sequences that are not specified by humans? To be widely applicable, the RL agent should also be able to adapt to diverse new system designs without substantial changes to the RL environment. Our experimental results suggest that such autonomous explorations are indeed possible.

We believe that the RL-based approach has the potential to enable a more systematic and rigorous evaluation of system security. We envision the RL framework to be used for both 1) studying potential security vulnerabilities of a system design and 2) evaluating the robustness of a defense mechanism. For example, AutoCAT can be used to automatically generate cache-timing attack sequences for a diverse set of cache configurations, replacement policies, or real processors. AutoCAT also tries to find attack sequences with higher success rates and bandwidth, providing a way to quantitatively compare the effectiveness of attacks across different cache designs. AutoCAT’s environment can be augmented with an explicit protection scheme such as an attack detector, and the RL agent can be asked to find an attack sequence that bypasses the defense. While AutoCAT cannot prove the security of a defense mechanism, testing a countermeasure with AutoCAT will provide a better measure of its robustness compared to only testing its effectiveness using the known attack sequences that it is designed for.

The following summarizes the main technical contributions and experimental findings of this paper:

- We present AutoCAT, the first framework to use RL to automatically explore cache-timing attacks. The framework can interface with a cache simulator or a real processor.
- We demonstrate that AutoCAT can find cache attack sequences for multiple cache configurations, replacement policies, and prefetchers. AutoCAT can also find attack sequences on multiple real processors with unknown replacement policies quickly, while for a human to adapt known attacks requires significant reverse-engineering.
- We demonstrate that AutoCAT can bypass several cache-timing defense and detection schemes, such as the partition-locked (PL) cache [81], detection based on the victim misses [4], [15], [36], [46], [95], detection based on autocorrelation [12], [88], and ML-based detectors [24].
- We present a novel cache-timing attack, named *Stealth-Streamline*, discovered by AutoCAT, which avoids detection based on the miss counts and has an up to 71% higher bit rate than existing LRU-based attacks on real machines.

We plan to make the artifact of AutoCAT publicly available on <https://github.com> under an open-source license.

## II. BACKGROUND AND MOTIVATION

### A. Cache-Timing Attacks

The cache timing channel is a widely-studied vulnerability in modern microprocessors, given its practicality and high bit rate. Depending on the threat model, it can be used as a side channel (where an attacker and a victim are non-cooperative) or a covert channel (where a sender and a receiver cooperate)

TABLE I: Actions/observations in known cache timing attacks.

Attack Category	Attacker’s actions	Victim’s actions	Observations
prime+probe [43]	access addr	access an addr	attacker’s latency
flush+reload [92]	flush addr	access an addr	attacker’s latency
evict+reload [53]	access addr	access an addr	attacker’s latency
evict+time [7]	access addr	access addresses	victim’s latency

on a shared cache to steal or send information. Without loss of generality, we assume a side channel scenario.

The cache-timing channels usually involve two parties, the attacker and the victim. A victim has a secret, and the memory operation of the victim depends on the secret. An attacker’s goal is to guess the secret without directly accessing the secret. The attacker needs to achieve the goal by making memory accesses and measuring the timing of the memory accesses or the victim’s external activities, e.g., using the timing/cycle measurement facilities such as RDTSCP in x86. The timing of a memory access indicates whether a cache line is in the cache or not. For example, in a prime+probe attack, the victim’s memory access will evict the attacker’s cache line from the cache, causing latency changes in the attacker’s future memory accesses. Thus, the attacker can infer the victim’s memory operation from timing observations.

The recent cache timing-channel models [17], [82] divide the attacks into three essential components, including the attacker’s actions, the victim’s actions, and the attacker’s observations. The attacker’s actions include normal memory accesses, cache line flushing, etc. The victim’s action is usually a secret-dependent memory operation such that it changes the state of the cache, e.g., accessing a secret address ( $addr_{secret}$ ). For the attacker’s observations, the attacker accesses certain cache lines and obtains the timing measurement to gain information about the secret ( $addr_{secret}$ ). With correct combinations, the attacker can learn the secret, as demonstrated in known attacks such as prime+probe [43], flush+reload [92], evict+time [53], cache collision [7] attacks, and other recent cache timing-channel attacks. Table I summarizes the actions of the common cache timing-channel attack categories [17], [26]. Other cache timing attacks also share the same set of actions and observations.

In this paper, we refer to a sequence of actions such as memory accesses, cache flushing, allowing a victim’s execution, and others in an attack on a specific system as an attack sequence. An attack category or strategy is a broader class of attack sequences that can be adapted to multiple systems, similar to the ones in Table I.

### B. Challenges of Cache-Timing Attack

For security analysis and testing, given a hardware design, we need to analyze the vulnerabilities and generate attack sequences to exploit these vulnerabilities. Many attack sequences may belong to a previously known attack category, while there may also be new attack sequences. Even for known attacks, there is a need to adapt those to the given design to test the effectiveness and bit rate of the attack [80]. In general, a cache timing attack involves (1) reverse-engineering the behavior of target microarchitecture design, (2) designing attack sequences to exfiltrate information, and (3) improving the signal quality in practice.

AutoCAT aims to address the challenges in the first two steps by focusing on reverse-engineering and attack sequence exploration when new or blackbox hardware is given. For other practical challenges in developing end-to-end attacks, such as building an accurate timer, reducing background noise, synchronizing the victim process, we leverage the existing techniques in the literature [65], [79], [86], [89]. The following discusses some of the main challenges in the attack steps.

A cache contains many design options, such as a replacement policy [57], cache directory [89], cache prefetcher [14], [80], etc. The microarchitectural implementation details are often kept as proprietary information by chip designers. Cache operations can also be pseudo-random such as random replacement policies, meaning the cache behavior is not entirely predictable. Reverse engineering effort can be onerous and only reveals limited information [3], [79]. For example, it could take up to 100 hours to reverse-engineer a replacement policy [79].

Some of the microarchitecture states are not directly measurable by timing. The attacker has to encode and decode the secret in such states, potentially resulting in complex and long attack sequences. For example, known attacks that make use of the cache replacement states and cache coherent states all require complex sequences of actions [9], [16], [86], [91], making it challenging to manually reason about an exploitable vulnerability and design an attack sequence.

To explore attacks in a given design, the above process needs to be repeated, which is laborious, and thus, tools helping attack explorations has been proposed. One method is to manually model the existing attacks in the cache [17], and then automatically generate attacks based on the model. However, so far, due to the complexity, such manual modeling methods [17], [26] are still limited to only the cache tag states, not including other cache states that could be vulnerable. Rigorous approaches can determine if certain security exploits exists in the design. However, formal methods [75] and information flow tracking [94] require whitebox modeling of the design, which in many cases is hard or impossible for a commercial microprocessor. In addition, lifting a new RTL-level design into a formal spec without manual effort is still challenging [28]. To deal with blackbox designs, fuzzing [20], [82] has been used to automatically generate attack sequences. However, to bound the size of the search space, fuzzing usually requires pre-defined attack sequences or predefined gadgets, which limit the attack strategies that can be explored. Ideally, we want less restrictions on the form of attack sequences and a tool that can explore (both known and unknown) attack sequences in blackbox designs.

### C. Reinforcement Learning (RL)

RL aims to find a policy that generates an action sequence that maximizes the long-term rewards. Figure 1 shows the high-level components and concepts in RL. First, there is an *RL agent*, which is controlled by a *policy*. There is an *environment*, which the RL agent interacts with. In each step, the RL agent takes an *action*, which feeds into the environment. The environment changes the state with the action, then exposes

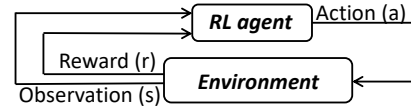


Fig. 1: RL formulation. RL agent does not need the knowledge of the internals of the environment to learn a policy.

observations to the RL agent, and assign *reward* values to the RL agent. The environment can optionally have a state where the environment state is reset. We call the sequence between two adjacent resets an *episode*. The goal of RL agent training is to generate a sequence of actions within an episode so that the sum of the rewards within one episode is maximized.

Recently, RL has been shown to learn human-level (or even super-human-level) policies in many game environments [47], [69] where there are well-defined rules and win/loss conditions. Those games are relatively light-weight and can be simulated easily. RL even discovers novel tactics, including novel openings in the game of Go [70], which humans have played for thousands of years. Similarly, cache-timing attacks can be formulated as a *guessing game*, where an attacker aims to guess a victim’s secret correctly while paying a small penalty (negative reward) for each cache access before making a guess.

The RL-based cache-timing attack discovery has several advantages over the alternatives. First, the RL formulation imposes few restrictions on the length of an attack, allowing flexible exploration of a broader set of attack sequences compared to the existing tool [82]. Second, RL is agnostic to the implementation of the environment as long as the interface including the action, reward and observation is provided. Thus, RL can work with both existing simulators as well as commercial processors without finding a formal white-box model of their caches [75]. Third, the RL is parameterized with neural networks, which can generalize to unexplored states and make smart decisions [39], [49], compared to random test-case generations that need to explore each state independently. Thus, RL can be more efficient in searching for vulnerabilities.

## III. AUTOCAT OVERVIEW

### A. Overview of AutoCAT Framework

Figure 2(a) shows the AutoCAT’s overall framework. A target cache implementation, the attacker and victim configuration, and the RL configuration is consumed by the AutoCAT’s RL engine for attack sequence generation. The cache implementation can be either a simulator (with a certain cache configuration) or a real hardware processor. The attack sequence is the sequence of memory operations, which can then be used in attack analysis by human experts to classify and identify potential new attacks. The attack sequence from the RL engine can also be used in an attack demonstration on real hardware. In this study, we manually analyzed the attack sequences to categorize them and applied a new attack sequence from AutoCAT to multiple Intel processors for real-world demonstration.

### B. High-level RL Engine Formulation

Figure 2(b) shows the formulation of cache guessing game as an RL problem in AutoCAT RL engine. In this setting, we

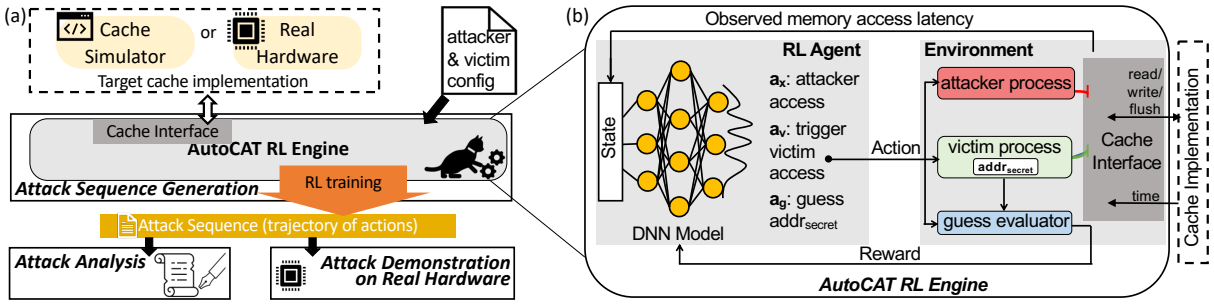


Fig. 2: (a) AutoCAT Framework. (b) AutoCAT RL Engine.

let the RL agent play the attacker role to explore possible attack strategies by controlling the attacker process. For simplicity, AutoCAT currently allows the RL agent to also control when the victim process runs. The RL agent is a policy parameterized by a deep neural network (DNN) model. The environment interact with a cache implementation, which handles the memory accesses of both the victim process and the attacker process. The environment also contains  $addr_{secret}$  which is the secret of the victim, and a guess evaluator to check if a guess is correct. Below we explain the RL formulation.

**Episode:** In each episode, the environment randomly generates the victim’s secret address ( $addr_{secret}$ ). The agent can then explore different actions and get observations. When the agent decides to make a guess on  $addr_{secret}$ , the episode will terminate. Reward will be given based on the guessing result and the number of actions taken.

**Rewards:** As the goal is to let the agent learn how to guess  $addr_{secret}$  correctly, we set the environment to return a positive reward if the agent’s guess is correct, and a negative reward if the agent makes a wrong guess. To encourage the agent to optimize the attack strategy (i.e., minimize the number of steps), we give a small penalty on each step the agent takes.

#### Actions:

- $a_X$ —access X where X is the memory address accessible by the attacker. As the attacker, the agent can access a cache line of address X, and observe a hit/miss.
- $a_v$ —trigger victim. The attacker can trigger the victim’s secret access; the victim accesses  $addr_{secret}$ , which potentially changes the cache state.
- $a_{gY}$ —guess that the value of  $addr_{secret}$  is Y where Y is chosen from address accessible by the victim, and end the current episode.

**Observations:** When the agent takes  $a_X$  (access X) above, the cache implementation conducts the memory operation, i.e., looks up the address X in the cache, returns the latency of the access, and updates the cache state. For  $a_v$  (trigger victim), the environment uses the  $addr_{secret}$  of the current episode and lets the cache simulator access  $addr_{secret}$ . With this environment, the agent can explore attacks using a combination of actions.

## IV. DESIGN AND IMPLEMENTATION

### A. Cache Implementation and Configuration

As depicted in Figure 2, there are two choices for cache implementation: a cache simulator written in software or a real

processor. The cache simulator allows quickly prototyping and implementing existing and new cache designs for vulnerability exploration. Exploring attacks on real hardware enables applying AutoCAT to real-world system designs even when their design details are not known.

**Cache simulator:** we embed an open-source cache simulator in Python [1] as the cache model in the AutoCAT framework. The cache configuration options are in Table II. We implement LRU, random [41], PLRU [72], and RRIP [29] replacement policies in the cache simulator. The cache simulator can be further extended to multi-level caches. For simplicity, we currently use physically-indexed physically-tagged (PIPT) caches and let the attacker and the victim directly use physical addresses for their accesses.

**Real hardware:** we leverage CacheQuery [79], a open-source tool to directly measure the cache access timing on Intel processors. CacheQuery automatically figures out the address mappings for L1, L2 and L3 caches and provides access to a specific cache level, without disabling prefetching, turbo Boost, frequency scaling, etc., which is close to real world operating conditions. Currently, CacheQuery [79] supports timing measurements for access sequences to one cache set.

Even though AutoCAT can interact with an arbitrary number of sets if the cache interface allows, our experiments focus on exploring attacks within small number of cache sets under different configurations, given that cache-timing attacks usually exploit the contention in each cache set independently.

### B. Attacker and Victim Configurations

Cache-timing attacks also depend on how the memory space is shared between an attacker and a victim, and which cache operations are available. For example, if there is no shared memory between the victim and the attacker, the flush+reload attack is not possible, but a prime+probe attack is still possible. We refer to these choices as the attacker and victim configurations. In our setting, for victim’s access, the agent will not get the latency of that step (N.A. as the observation), assuming victim access latency is not directly visible to the attacker. To allow exploring attacks with and without shared memory space between the attacker and the victim, the address range of the victim and the address range of the attacker are configurable in AutoCAT, as listed in Table II. These address ranges determine whether the attack process can touch the same addresses accessed by the victim. In addition, cache-line flush instruction (`clflush` in x86) is not always

TABLE II: AutoCAT configuration parameters.

Option Type	Option Name	Definition	Type	Range
Cache configs in cache simulator	num_blocks	total number of blocks in the cache	integer	2,4,...
	num_ways	number of ways of the cache	integer	2,4,6,8,12, 16
	rep_alg	replacement algorithm for all cache sets	str	"lru", "plru", ...
Attacker and Victim configs	attacker_addr_s	starting address of attacker	integer	0,1,2,3,...
	attacker_addr_e	end address of the attacker	integer	0,1,2,3, ...
	victim_addr_s	starting address of victim	integer	0,1,2,3,...
	victim_addr_e	end address of the victim	integer	0,1,2,3,...
	flush_enable	whether to enable flush instruction for the attacker	boolean	true, false
	victim_no_access_enable	whether the victim need to make a memory access when triggered by the attacker	boolean	true,false
RL config	detection_enable	whether the episode terminates when the attack detector signals a potential attack	boolean	true,false
	window_size	size of the history window in the observation space	integer	1,2,3, ...
	correct_guess_reward	reward when the attacker makes a guess and the guess is correct	float	(0, $\infty$ )
	wrong_guess_reward	reward when the attacker makes a guess and the guess is wrong	float	( $-\infty$ , 0)
	step_reward	reward when the attacker make a memory access	float	( $-\infty$ , 0)
	length_violation_reward	reward value when the length of episode exceed limit	float	( $-\infty$ , 0)
	detection_reward	reward when the attack detector signals a potential attack	float	( $-\infty$ , 0)

available, *e.g.*, in JavaScript. We make `flush_enable` a configuration option in AutoCAT.

In many cache timing channels, rather than encoding the information with different addresses, whether the victim has made an access or not also leaks information, *e.g.*, prime+probe. To explore this scenario, we use the `victim_no_access_enable` option, and use `addr_secret_e` to represent the victim makes no access when triggered. When this is enabled, the victim can access one of the addresses in the victim’s address space or make no access (`addr_secret_e`) with the same probability. To explore attacks with a detection scheme, we have the configuration option `detection_enable`, which terminates an episode when the sequence is recognized as an attack by the detector.

### C. RL Engine and Configuration

**RL Action Space.** The RL agent can have the attack software take one of the three actions (*i.e.*,  $a_X$ ,  $a_v$ ,  $a_{gY}$ ), as discussed in Section III-B. If `flush_enable` is set, we extend the action  $a_X$  to also include cache line flush denoted by  $a_{fX}$ . Similarly, if `victim_no_access_enable`, we use  $a_{gE}$  to denote that the agent guesses that the victim made no access after triggered. When the attacker makes a guess, it can be either  $a_{gY}$  or  $a_{gE}$ . Overall, the RL agent can take one action for each step: 1) access/flush:  $a_X$  or  $a_{fX}$ ; 2) trigger victim:  $a_v$ ; 3) guess:  $a_{gY}$  or  $a_{gE}$ , depending on the attacker/victim configuration. We use one-hot encoding to represent the actions.

**RL State Space.** For its own memory access  $a_X$ , the attacker can directly observe the cache access latency in terms of a hit or a miss. To provide more information to let the RL agent learn efficiently, we encode a state incorporating the history of actions and observations, and compose the state space  $S$  as a Cartesian product of subspaces, as follows:  $S = \prod_{i=1}^W (S_{lat}^i \times S_{act}^i \times S_{step}^i \times S_{trig}^i)$ , where  $S_{lat}^i$ ,  $S_{act}^i$ ,  $S_{step}^i$ ,  $S_{trig}^i$  are the subspaces representing the access latency, an action taken, the current step, and whether the victim has already been triggered at step  $i$ .  $W$  is the window size that can be set using `window_size`. Empirically we set it to be 4-8 times `num_blocks`. The latency subspace  $S_{lat}^i$  is defined as  $S_{lat}^i = \{s_{hit}, s_{miss}, s_{N.A.}\}$ , representing hit/miss and N.A. states. The action subspace  $S_{act}^i$  is defined as  $S_{act}^i = \{s_a | a \in \{a_X, a_{fX}, a_v, a_{gY}, a_{gE}\}\}$ , representing the state in which action  $a$  is taken at step  $i$ . The step subspace  $S_{step}^i$  is defined as  $S_{step}^i = \{s_{step1}, s_{step2}, \dots\}$ . The victim triggering subspace  $S_{trig}^i$

is defined as  $S_{trig}^i = \{s_t, s_m\}$ , representing whether the victim has been triggered or not. The RL agent uses this information in order to make a guess after the secret-dependent memory access by the victim is triggered.

For real hardware, having the agent interact with hardware for each action is slow and also makes the training more susceptible to system noise. To address this challenge, for training on real hardware, we execute all instructions in an episode together as a batch. The latency subspace is masked until the agent make a guess, when all instructions within an episode are executed and latency of memory accesses are revealed.

**RL Algorithm and DNN Model** In this paper, We use proximal policy optimization (PPO) [67] since it typically performs similarly or better than other methods while being much simpler to tune [2]. For most experiments, we use a multi-layer perceptron (MLP) [25] to encode our RL policy. The input states, encoded as one-hot vectors, are sent to two hidden layers, each with 256 neurons and `tanh` activation, followed by a softmax that outputs action probability. In certain scenarios, we also use a Transformer [77] model (input feature dimensions 128, 1 layer encoder, 8-head, FFN dimension 2048) to learn step-wise representation, followed by average-pooling over steps for sequence embedding. Other recurrent models like LSTMs [27] or RNNs can also be used but may be more difficult to tune.

**Reward Configuration.** When the agent makes a guess  $a_{gY}/a_{gE}$ , depending on whether the guess is correct or not, our environment assigns the reward `correct_guess_reward` or `wrong_guess_reward`. For all the actions taken by the RL agent (*e.g.*,  $a_X$ ,  $a_{fX}$ ,  $a_v$ ), the environment assigns a negative `step_reward` to encourage the agent to find short attack sequences. These rewards are listed in Table II. PPO is not very sensitive to the reward value combinations and we use the following rewards for the experiments: `correct_guess_reward` = 200, `wrong_guess_reward` = -10,000, and `step_reward` = -10. We also explored other reward value combinations in Appendix A. Once the sum of the reward within a episode is converged to a positive value, we use deterministic replay to extract the attack sequences. To discourage the RL agent from taking too many steps without making a guess,

we have `length_violation_reward`, which is a large negative value when the length of an episode is longer than `window_size`. When we implement a detection scheme in the environment, there is also the `detection_reward` which is the reward (negative value) when the sequence is caught by the detector as a potential attack.

#### D. Attack Analysis and Demonstration

Once the attack sequence is generated using the RL engine, it can be further analyzed and demonstrated. First, for attack analysis, given a particular sequence, we want to know what is the type of the attack, and whether is it a new type of attack. Currently, we rely on human inspections to classify attacks and identify new attacks. Automated classification and identification of the attack sequences is an orthogonal problem and we left it as future work. With the attack sequences generated by AutoCAT, we can demonstrate them in real hardware. We embed the attack sequence into a assembly template, which uses pointer chasing to perform measurement of timing of one address [85]. With the assembly code corresponding to the attack sequence, we can then measure the bit rate and the error rate of the attack on a real processor with realistic noise.

### V. EVALUATION AND CASE STUDIES

In AutoCAT, we use RLlib [40] and RLMeta [90] as the RL frameworks to train the RL agent. Our DNN model is implemented in PyTorch [56]. The RL engine follows the gym [10] interface. We implement the cache simulator based on [1]. The RL training process is performed on a machine with an Intel Xeon CPU E5-2687W v2 running Ubuntu 16.04 and Nvidia K80 GPUs with CUDA 10.2.

#### A. Attacks on Real Hardware

AutoCAT can explore attack sequences on real hardware without explicitly knowing all the architectural details, including associativity, replacement policies, frequency scaling, hardware prefetching, and other undocumented features. In our experimental setup using CacheQuery [79], the attacker and the victim run in a single process on the same core. We experimented with multiple cache levels from three different processors, all with the same attacker and victim configurations where the attacker needs to guess whether the victim accesses the cache set or not. The configurations and attack sequences found by AutoCAT are shown in Table III. The table also shows the accuracy for each attack sequence based on repeating the sequence 1,000 times on the same processor using CacheQuery. Due to noise in real processors, the accuracy is slightly lower than 100%.

The results show that AutoCAT is able to find attack sequences on real processors, without explicitly specifying the number of ways or reverse engineering the replacement policies, prefetchers, etc. Such information is usually needed by human experts to adapt known attacks. For example, to demonstrate prime+probe, one needs to understand the replacement policy to prime and also probe a cache set efficiently [80]. However, the replacement policies of recent

processors are rarely documented publicly by the vendor and difficult to precisely reverse engineer [79]. Even though it is possible to reverse engineer an unspecified replacement policy from a real world processor, it takes significant amount of time (as long as 100 hours) and then one still needs to develop attack sequences manually. AutoCAT can find effective attack sequences within *several hours* in our experiments. The attack sequence found by AutoCAT is consistent with the reverse engineering result from the previous study [79], where each address has to be accessed twice to set the reference count of the corresponding cache block to zero.

#### B. Attacks on Diverse Cache/Attack Configurations

The flexibility of the cache simulator allows us to study diverse cache and attack configurations more easily. To evaluate how effective the RL agent can be across a broad range of environments, we tested AutoCAT under many different cache and attacker/victim configurations shown in Table IV. These environments use the (true) LRU replacement algorithm by default. Note that the attacker/victim configuration limits the feasible attacks in the environment. For example, if the environment does not allow the cache flush instruction, the flush+reload attack is not possible. If there is no shared address space, flush+reload or evict+reload is not feasible. The expected attack categories for each configuration are also listed in Table IV.

The RL agent could successfully find working attack sequences for all configurations we tested. Table IV shows one example attack sequence for each configuration that was automatically found by the RL agent. The RL-generated attack sequences vary for different environment configurations and cover a range of known attack categories, including prime+probe, flush+reload, and evict+reload. For configuration 1 and 3-7, we use the MLP model for the RL agent. For configuration 2 and 8-14, we use a Transformer model in RLMeta framework.

In most cases, the RL agent generates attack sequences that are of the attack type expected for the configuration. Interestingly, the attack sequence found by the agent can be more efficient than the attack we expected. In some cases, the RL agent can generate a shorter sequence than expected. For example, for configuration 1 in Table IV, a textbook prime+probe attack will result in the following attack<sup>1</sup>:  $4 \rightarrow 5 \rightarrow 6 \rightarrow 7 \rightarrow v \rightarrow 4 \rightarrow 5 \rightarrow 6 \rightarrow 7 \rightarrow g$ . Meanwhile, the attack sequence given by AutoCAT is:  $5 \rightarrow 4 \rightarrow 7 \rightarrow v \rightarrow 5 \rightarrow 7 \rightarrow 4 \rightarrow g$ . The RL agent removes the unnecessary memory access in the textbook prime+probe attack, i.e., by attacking three cache sets, the attacker can already learn which of the four possible addresses the victim accessed. For configurations 5 and 7 in Table IV, instead of a prime+probe attack, the RL agent found a shorter attack sequence leveraging the LRU state. However, the attack sequences found by AutoCAT are not always the shortest in length (e.g., configuration 6 in

<sup>1</sup>For brevity, we only use the subscript  $i$  of an action  $a_i$  to represent the action. For example, to represent accessing address 3, we directly use 3 to represent  $a_3$ .

TABLE III: Attack sequence found using AutoCAT on real hardware.

CPU	Cache level	#Ways	Rep. Pol.	Victim addr.	Attacker addr.	Example attack sequence found by AutoCAT	Accuracy	Attack Category
Xeon E5-2660v3 (Haswell)	L1	8	PLRU	0/E	0-8	2 → 1 → 5 → 6 → 4 → 4 → 7 → 8 → 4 → 8 → v → 3 → 4 → v → 0 → g	0.999	LRU
	L2	8	PLRU	0/E	0-8	1 → 8 → 2 → 3 → 4 → 7 → 2 → 5 → 4 → 2 → 8 → 6 → v → 6 → 3 → 6 → 7 → 1 → g	0.999	LRU
Core i7-6700 (SkyLake)	L1	8	PLRU	0/E	0-8	1 → v → 4 → v → 5 → v → 5 → 5 → 3 → 8 → 4 → v → 0 → 2 → 0 → 1 → v → 8 → 4 → v → g	0.996	LRU
	L2	4	N.O.D.†	0/E	0-8	0 → 1 → 7 → 3 → 6 → 6 → 6 → v → 5 → 0 → 4 → 1 → 7 → 5 → g	0.997	LRU*
	L3	4†	N.O.D.	0/E	0-8	v → v → 4 → 0 → 5 → 1 → 1 → 4 → 2 → 7 → 3 → 3 → v → v → 3 → 0 → g	1.0	LRU*
Core i7-7700K (KabyLake)	L3	8†	N.O.D.	0/E	0-8	... → 3 → v → 3 → v → 6 → 7 → 3 → 3 → 5 → 1 → 5 → 1 → 6 → g	0.966	LRU*
	L3	4†	N.O.D.	0/E	0-8	1 → 2 → 6 → 6 → 8 → 8 → 8 → v → 0 → g	1.0	LRU*
Core i7-7700K (KabyLake)	L3	8†	N.O.D.	0/E	0-8	7 → 7 → 3 → 4 → 6 → 0 → 2 → 1 → 6 → 5 → 3 → 2 → v → 5 → 4 → 1 → 2 → 8 → v → 8 → 7 → 6 → 6 → 3 → 3 → 4 → g	0.991	LRU*

† indicates way partition using Intel CAT. ‡ Not Officially Documented. \* Attacks based on replacement states, but with different sequences due to the replacement policy.

TABLE IV: The RL environment configurations tested, and the example attack sequences generated by AutoCAT.

No.	Cache config.			Attacker& victim config.			Expected attacks	Example Attack found by AutoCAT	
	Type†	Ways used	Sets	Victim addr	Attacker addr	Flush inst		Possible attacks‡	Attack sequence (p indicates prefetch)
1	DM	1	4	0-3	4-7	no	PP	5 → 4 → 7 → v → 5 → 7 → 4 → g	PP
2	DM+PFnextline	1	4	0-3	4-7	no	PP	6(p7) → 4(p5) → v → 4(p5) → 5(p6) → g	PP
3	DM	1	4	0-3	0-3	yes	FR	... → f1 → v → 1 → f0 → v → f2 → v → 2 → f3 → 0 → g	FR
4	DM	1	4	0-3	0-7	no	ER, PP	... → 3 → 7 → 4 → 6 → v → 3 → 0 → 6 → 4 → g	ER and PP
5	FA	4	1	0/E	4-7	no	PP, LRU	4 → 6 → 7 → v → 5 → 4 → g	LRU
6	FA	4	1	0/E	0-3	yes	FR, LRU	0 → 3 → 1 → 2 → f0 → 2 → v → 3 → 0 → g	FR
7	FA	4	1	0/E	0-7	no	ER, PP, LRU	v → 4 → 1 → 6 → 7 → v → 1 → v → 5 → 6 → g	LRU
8	FA	4	1	0-3	0-3	yes	FR, LRU	f3 → f2 → v → 2 → 3 → f0 → v → 0 → g	FR
9	FA	4	1	0-3	0-7	yes	FR, LRU	f0 → f2 → f1 → v → 2 → 1 → 0 → g	FR
10	DM	1	8	0-7	0-7	yes	FR	f2 → v → 2 → f4 → f0 → v → 0 → 4 → f3 → f7 → v → 3 → v → 7 → f1 → f6 → v → 6 → 1 → g	FR
11	FA	8	1	0/E	0-7	yes	FR, LRU	f0 → v → 0 → g	FR
12	FA	8	1	0/E	0-15	no	ER, PP, LRU	7 → 11 → 10 → 5 → 4 → 2 → 3 → 1 → v → 0 → g	ER
13	FA+PFnextline	8	1	0/E	0-15	no	ER, PP, LRU	4 (p5) → 9 (p10) → 15 (p16) → 2 (p3) → v → 0 (p1) → g	ER
14	FA+PFstream	8	1	0/E	0-15	no	ER, PP, LRU	15 → 9 → 8 → 7(p6) → 11 → 6 → 12 → 14 → v → 0 → g	ER

† FA: fully-associative, DM:direct-mapped, PFnextline: nextline prefetcher, PFstream: stream prefetcher. ‡ FR: flush+reload, ER: evict+reload, PP: prime+probe.

Table IV) and may contain unnecessary accesses; nonetheless, they do capture the key mechanism that enables the attack for each configuration. In some cases, the sequence found by the agent is an interesting combination of different attacks, e.g., configuration 4 in Table IV results in an attack that is a combination of evict+reload and prime+probe, which could make attack detection and defense more difficult.

The cache configurations 2, 13, and 14 include either a next-line prefetcher [71] or a stream prefetcher [31]. The RL agent could find attack sequences even with prefetching.

### C. Case Study 1: Attacking Replacement Policy

AutoCAT’s cache simulator allows us to implement different replacement policies and address mappings in the same setting and the RL agent can adapt to them. We focus on replacement policy in this case study because recent attacks based on replacement states [9], [86] show long and complex sequences, and we want to demonstrate the effectiveness of AutoCAT. We use a 4-way cache (set) with four replacement algorithms: three deterministic (LRU, PLRU, and RRIP) and one non-deterministic (random). For a 4-way cache set, both LRU and RRIP keep 2-bit state information (ranging from 0-3) for each cache block, called *age* in LRU and *re-reference prediction value (RRPV)* in RRIP, which will be incremented correspondingly. The cache block with the largest state bits will be evicted upon a cache miss. In LRU, the most recently used cache block will be assigned *age*=0. In RRIP, a newly installed cache block will be assigned *RRPV*=2, and only upon a cache hit will it be promoted to *RRPV*=0. Pseudo-LRU implemented using a tree structure is a way of approximating LRU with less state information, whose behavior will be slightly different

from LRU. The attacker’s address space is configured to be from 0 to 4 (large enough to fill the 4-way cache set). The victim is configured to either access address 0 or make no access depending on a one-bit secret. The configuration is similar to that of configuration 6 in Table IV. The cache is initially accessed by address 0 and 1 before the attack.

As shown in Table V, the RL agent can successfully generate valid attack sequences for all three deterministic policies, which takes less than one hour of RL training for each case. For the deterministic replacement policies, RL finds attacks that always make a correct guess (there is no noise). The results also show that PLRU and RRIP need longer training and a longer attack sequence compared to LRU. In the RRIP attack example, the 3 → 2 → 3 → 1 sequence is needed to ensure that for both address 1 and address 3, *RRPV* is 0 since they are cache hit and predicted to be immediately re-referenced. For address 2, *RRPV* is 2 since it is not re-referenced. As shown in Figure 3, the victim access of address 0 will set *RRPV*=0 for address 0 and leaving address 2 to be replaced. When triggered, regardless of whether the victim accesses 0 or not, there is no miss event, which is similar to the RELOAD+REFRESH [9] attack reported recently.

Unlike a deterministic replacement policy where the next state will be fully determined given the action and current state, the next state is hard to predict in the (pseudo)-random replacement algorithm. Thus, an attack sequence that results in a correct guess may result in a wrong guess in another evaluation. The RL agent can also produce different actions depending on the current observation. In that sense, unlike a deterministic replacement policy, there is no single attack sequence that always works in the random replacement policy,

TABLE V: RL training statistics and generated attacks for deterministic cache replacement policies.

Repl. alg.	Steps to converge	Episode length	Attack sequence found by AutoCAT
LRU	296,000	6.59	$v \rightarrow 4 \rightarrow 3 \rightarrow 2 \rightarrow 0(\text{hit/miss}) \rightarrow g$
PLRU	340,000	9.14	$1 \rightarrow v \rightarrow 1 \rightarrow 4 \rightarrow v \rightarrow 3 \rightarrow 2 \rightarrow 1(\text{miss/hit}) \rightarrow g$
RRIP	336,000	9.68	$3 \rightarrow 2 \rightarrow 3 \rightarrow 1 \rightarrow v \rightarrow 4 \rightarrow 2(\text{miss}) \rightarrow g0; 3 \rightarrow 2 \rightarrow 3 \rightarrow 1 \rightarrow v \rightarrow 4 \rightarrow 2(\text{hit}) \rightarrow 0 \rightarrow gE$

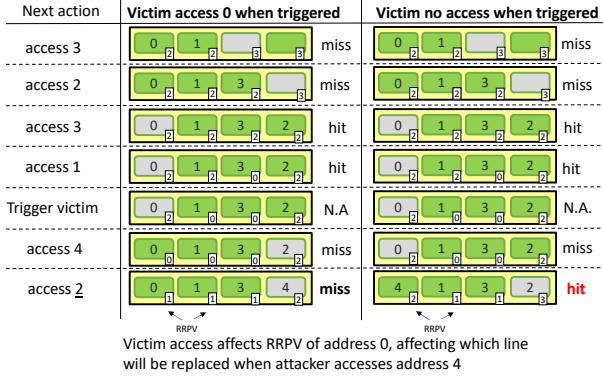


Fig. 3: Attack sequences and corresponding cache state for RRIP replacement algorithm and victim access (left)/no access (right) information is inferred by the attacker. Gray blocks indicate the one to be evicted on a cache miss.

whose eviction rate depends on the number and the sequence of memory accesses. Instead, we evaluate the attack accuracy of the RL agent over 2,000 evaluation runs. As shown in Table VI, the step reward determines the tradeoff between the attack length and the accuracy. The evict+reload strategy is similar to the prior attack on random replacement policy [41].

#### D. Case Study 2: Bypassing Defense and Detection Techniques

To protect against cache timing-channel attacks, a variety of detection and mitigation techniques have been proposed. AutoCAT’s cache simulator can also be used to test research prototypes of defense and detection mechanisms proposed in previous works that lack actual real processor implementations. This is especially useful when evaluating new protection or detection schemes and find vulnerabilities. We implemented four cache timing-channel protection schemes in the cache simulator: 1) Partition-locked (PL) cache [81], 2) Hardware Performance Counter (HPC)-based detection [4], [15], [36], [95], 3) Autocorrelation-based detector similar to CC-hunter [12] and, 4) machine learning-based detector similar to Cyclone [24]. AutoCAT successfully finds attack sequences that can bypass these protection schemes.

**Partition-Locked (PL) Cache.** PL cache [81] provides special instructions to lock specific cache lines in a cache to prevent them from being evicted. The victim program can lock its own cache lines so that they cannot be evicted by the attacker program. Further, the victim’s access to the locked cache lines will not evict any of the attacker’s cache lines. In [26], the formal analysis on a simplified cache model concludes that PLcache is secure when the attacker and the victim do not share address space.

We implemented the PL cache with the lock/unlock interface in our cache model. To use the PL cache as a defense

TABLE VI: The RL-generated attacks on the random replacement policy.

Step reward	End accuracy	Episode length	num of sequences
0	1.0	41.00	737
-10	0.87	35.75	171
-20	0.999	34.99	163
-30	0.897	30.17	122

TABLE VII: Comparison of PLRU w/ and w/o PLCache.

Cache	Steps to converge	Episode length
PLCache	232,000	11.66
baseline	176,000	8.58

TABLE VIII: Bit rate, autocorrelation, and accuracy of attacks.

sampled attacker	bit rate (guess/step)	max autocorrelation	accuracy
textbook	0.1625	0.96	1
RL_baseline	0.236	0.92	0.99
RL_autocor	0.1975	0.55	0.99

mechanism, we assume the victim’s cache line is pre-installed and locked in the cache. We use a 4-way cache, and the address range of the attacker is 1-5 and the victim either accesses 0 or has no access depending on the secret value. The setting is considered to be secure in [26]. For this setting, the training takes about 45 minutes. Table VII shows the training time (# of steps) and the attack sequence length for a cache with PLRU, with and without the PL cache. AutoCAT successfully found an attack that works even with the PL cache, represented by attack sequence  $1 \rightarrow v \rightarrow 3 \rightarrow 3 \rightarrow 2 \rightarrow 5 \rightarrow 5$ . In this attack, the victim’s cache line (address 0) always stays in the cache, and the victim’s behavior (whether the victim makes access or not) does not evict any of the attacker’s cache lines. However, the victim’s access affects the LRU state. When the attacker made subsequent accesses, it can tell whether the victim accessed address 0 or not by observing if a new block can be brought into the cache. This attack is reported in recent literature [86].

**Autocorrelation-based Detection.** Autocorrelation of cache events have also been proposed as a way to detect the existence of cache-timing channels [12], [88] based on the observation on the common covert-channel sequences. In CC-Hunter [12], two types of conflict miss events (i.e., victim evicting attacker’s cache line,  $V \rightarrow A$ , encoded with “0”, and attacker evicting victim’s,  $A \rightarrow V$ , encoded with “1”) are considered in the event train  $\{X_i\}$  where  $0 \leq i \leq n$ , and  $n$  is the length. In a contention-based cache side channel like prime+probe, these two events are interleaved periodically. We can check the autocorrelation  $C_p$  at lag  $p$  using the following equation:  $C_p = \frac{\sum_{i=0}^{n-p} (X_i - \bar{X})(X_{i+p} - \bar{X})}{\sum_{i=0}^n (X_i - \bar{X})^2}$ . If there exists  $p$  where  $1 \leq p \leq P$  ( $P$  is a predefined parameter) such that  $C_p > C_{threshold}$  (e.g. 0.75), then it is considered to be an attack.

For example, in a 4-set direct-mapped cache where the victim and attacker’s address space is 0-3 and 4-7, a “textbook” prime+probe attack would perform the following steps. First the address space 4-7 is primed by the attacker, after that one victim access is triggered, and then addresses 4-7 are probed. The event train and the corresponding autocorrelogram is shown in Figure 4. The maximum autocorrelation for  $p \geq 1$  is 0.96, which is over the threshold.

The AutoCAT generated baseline sequence ( $RL\_baseline$ )

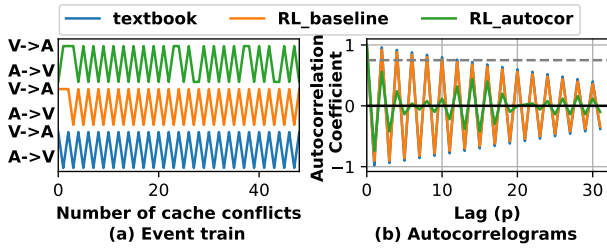


Fig. 4: (a) Event train (A→V: attacker’s conflict misses with the victim and V→A: victim’s conflict misses with the attacker.) (b) Autocorrelograms of the event trains. The dashedline shows the threshold for detecting an attack.

can be also detected by this autocorrelation-based detector, as shown in the conflict miss event train and the autocorrelogram (Figure 4). The maximum autocorrelation for  $p \geq 1$  is 0.92. Note that the event train and the corresponding autocorrelograms will be different for each sample. However, we observe the maximum autocorrelation of 0.875-0.940 over 25 distinctive inferences (sampled from randomly generated victim addresses), which are all above the detection threshold.

However, AutoCAT can learn to bypass such autocorrelation detector if the reward of the RL agent is augmented to avoid high autocorrelation. We use  $L_2$ -penalty of  $C_p$  to penalize high autocorrelations, which is defined as  $R_{L_2} = a \sum_{p=1}^P \frac{C_p^2}{P}$  where  $a$  is a negative number and  $P \ll n$  is the length of  $C_p$  used for autocorrelation-based detection. The sampled cache conflict miss event train and the autocorrelogram of the resulting agent ( $RL\_autocor$ ) are shown in Figure 4. The maximum autocorrelation beyond lag 0 is 0.55 in this example. For 25 different samples, we observe the maximum autocorrelation of 0.396-0.772 with only 2 samples over 0.75. The results indicate that the agent ( $RL\_autocor$ ) will be able to evade autocorrelogram detection with high probability.

Table VIII compares the attack sequence from the textbook,  $RL\_baseline$ , and  $RL\_autocor$  in terms of bit rate (average number of guesses per step), accuracy, and autocorrelation. All attacks achieve over 0.99 accuracy and the RL agents have a higher bit rate than the textbook attack. This is because the RL agents optimize the bit rate to gain higher rewards. We observe when a miss is already observed during a probe step, RL agents can guess the secret while the textbook attack still completes the remaining accesses. We also observe that the bit rate of  $RL\_autocor$  is lower than  $RL\_baseline$  because  $RL\_autocor$  makes additional accesses to reduce autocorrelation.

**ML-based Detection.** Machine learning classifiers can also be used for detecting cache-timing attacks. For example, in Cyclone [24], the frequency of cyclic access sequences by different security domains (e.g.,  $a \rightsquigarrow b \rightsquigarrow a$ ) for each cache line within each timing interval is used as the input of an SVM classifier to detect cache timing channels efficiently. We use a 4-set direct-mapped cache as an example and implement domain tracking and cyclic access sequence counting for each cache line following [24]. We train an SVM classifier using SPEC2017 benchmarks for benign memory access traces and the textbook prime+probe attack for malicious memory traces.

TABLE IX: Comparison of bit rate, guess accuracy and detection rate by the SVM.

sampled attacker	bit rate (guess/step)	attack accuracy	SVM detection rate
textbook	0.1625	1	1
$RL\_baseline$	0.228	0.990	0.907
$RL\_SVM$	0.150	0.964	0.021

The 5-fold validation accuracy of the SVM is 98.8%.

We then train the AutoCAT’s RL agent ( $RL\_SVM$ ) with this SVM detector. If the SVM detector correctly reports the existence of the attack, the RL agent gets a negative reward. We also train an  $RL\_baseline$  agent without detection penalty. We show the result in Table IX. The textbook and the  $RL\_baseline$  can be easily detected by the SVM detector, with the detection rate of 1 and 0.907, respectively. However, when the RL agent is trained with the SVM detection penalty, it can find attack sequences that can bypass the SVM detector, with the detection rate of 0.021, at the cost of a reduced bit rate. This indicates ML-based detector trained on static traces can be easily bypassed by an RL-based attacker and novel training method for ML-based detector is needed.

**$\mu$ arch Statistics-based Detection.** Most of the cache-timing attacks cause the victim’s process to incur more cache misses during the attack. Thus, detection schemes based on microarchitecture event counts/statistics have been proposed to leverage hardware performance counters (HPCs) to monitor the cache hit-rate of the victim process and detect an attack at runtime [4], [15], [36], [95]. More recently, [46] observes that fine-grained statistics can achieve better detection accuracy. When an abnormally large number of cache misses are observed, the detector signals a potential attack.

To evaluate the statistics-based detection scheme in AutoCAT, we consider the attack is detected when the victim access triggers a cache miss. We terminate the episode and assign a negative reward if the victim access results in its cache miss during training. This configuration encourages the RL agent to avoid victim misses, and thus, avoid the miss-based detection.

Figure 5(b) shows the attack sequence generated by AutoCAT for a 4-way cache with the miss-based detection scheme. This is a new attack sequence, which is a novel combination of the two recent attacks in literature (shown in Figure 5(a)). The attack sequence can be divided into sub-sequences, which are the LRU set-based or LRU address-based attacks [86]. The two sub-sequences overlap with each other in a way similar to the Streamline attack [65]. Based on the gray part of the sequence generated by AutoCAT in Figure 5(b), we construct a new attack, named *StealthyStreamline*, in Figure 5(c). Compared to the Streamline attack, the new *StealthyStreamline* attack does not cause cache misses of the victim process, thus is stealthier. Compared to the LRU-based attacks, *StealthyStreamline* has a higher bit rate by overlapping the steps for multiple bits, effectively transferring multiple bits at a time. Figure 5(d) illustrates the cache state when the *StealthyStreamline* is transmitting 2 bits. The attacker observes different timing when the victim has 4 different possible secret values.

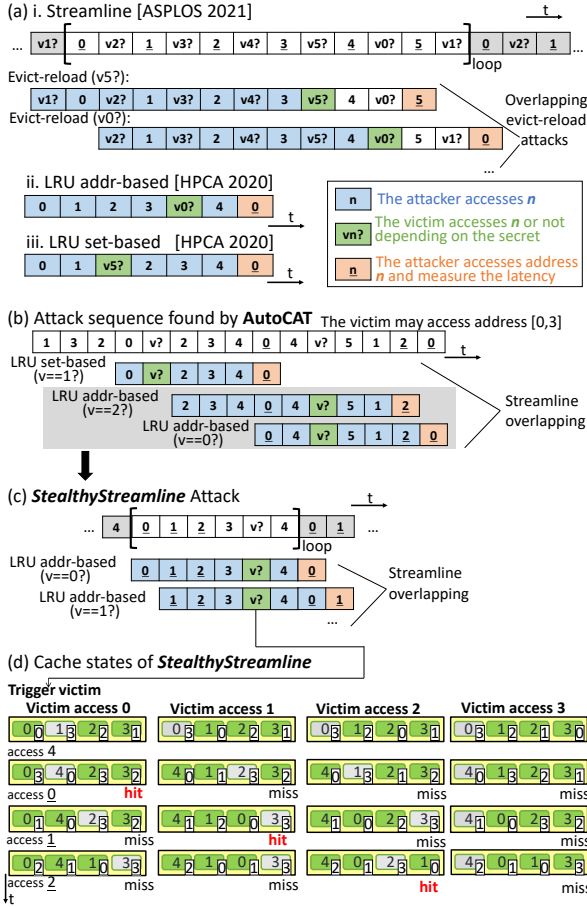


Fig. 5: *StealthyStreamline* attack. (a) Known attack sequences in the literature. (b) The new attack sequence found by AutoCAT, which can be seen as the combination of the two known attacks. (d) *StealthyStreamline* attack derived from the attack found by AutoCAT. (e) The cache state changes of the *StealthyStreamline* attack. The numbers in the right bottom corner indicate the LRU age of the cache line.

### E. Demonstration of Attacks on Real Machines

The attack sequence discovered by AutoCAT captures one essential aspect of real-world cache-timing attacks. However, the real-world attacks also have to deal with common practical issues like measurement noise, calibrations, interferences, etc. These practical issues are common in many attacks and people handle them in a similar way regardless of the actual attack sequences. To demonstrate the usefulness of these attack sequences in real-world scenario, we put the attack sequence from AutoCAT into an open-source attack assembly template [85], which handles calibration, measurement, cache line access, and forms a covert channel corresponding to the attack sequence. We can then execute the assembly on a real processor under a practical operating environment.

With this method, we demonstrate the *StealthyStreamline* attack sequence for a covert channel in the L1 data cache on four different Intel processors (Table X). Two processors have a 32KB (8-way) L1 data cache, and the other two latest

TABLE X: Covert channels on real machines.

CPU	$\mu$ -arch.	L1D config	OS	Bit Rate <sup>d</sup> (Mbps)		
				LRU	SS. <sup>b</sup>	Impr.
Xeon E5-2687W v2	IvyBridge	32KB(8way)	Ubuntu18	6.2	7.7	24%
Core i7-6700	Skylake	32KB(8way)	Ubuntu18	3.6	4.5	22%
Core i5-11600K	RocketLake	48KB(12way)	CentOS8	3.4	5.7	67%
Xeon W-1350P	RocketLake	48KB(12way)	Ubuntu20	2.1	3.7	71%

<sup>a</sup> The bit rate when the average error rate < 5%. <sup>b</sup>SS. for *StealthyStreamline*.

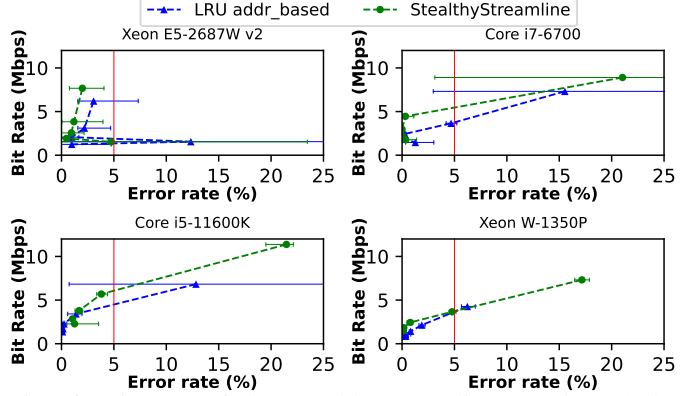


Fig. 6: Bit rate of the *StealthyStreamline* attack and the LRU address-based attack on four different processors. The horizontal error bars show the range of errors across different transmission runs.

processors employ a 48KB (12-way) L1 data cache. The machines run different versions of Linux.

We generalize the 2-bit *StealthyStreamline* attack sequence in a 4-way cache (in Figure 5) to 8-way and 12-way scenarios by adding extra accesses to the cache lines that map to the same cache set. We implemented both 2-bit (4 possible  $addr_{secret}$  values) and 3-bit (8 possible  $addr_{secret}$  values) *StealthyStreamline* covert channels.

**Bit Rate and Error Rate:** We test the bit rate and the corresponding error rate of the covert channel within a process. We do not change any system configuration with the purpose of facilitating the attack, *i.e.*, hardware prefetchers remain enabled. We measure the bit rate by measuring the time of sending a 2048-bit random string 100 times, using `time` in Linux. We evaluate the error rate using the Hamming distance between the message being sent and the message received. We observe that the 3-bit *StealthyStreamline* has a high error rate due to the tree structure in PLRU, while the 2-bit *StealthyStreamline* has a low error rate.

Figure 6 shows the bit rates and the corresponding error rates for the 2-bit *StealthyStreamline* covert channel and the baseline LRU address-based covert channel. In most of the machines, we observe the LRU address-based covert channel has a larger variation in the error rate across different experiment runs, as shown by the error bars in Figure 6. For the error rate less than 5%, *StealthyStreamline* has a higher bit rate than the LRU address-based covert channel. In an 8-way cache, *StealthyStreamline* has up to a 24% higher bit rate. In the latest 12-way cache, the *StealthyStreamline* has up to a 71% higher bit rate. *StealthyStreamline* improves the bit rate more for caches with a higher associativity, because a smaller fraction

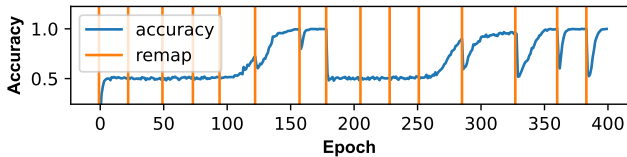


Fig. 7: Attack accuracy as a function of training epochs, the orange vertical lines show when the remapping happens.

of memory accesses (4 out of 10 for the 8-way cache vs. 4 out of 14 for the 12-way cache) need to be measured and measuring the latency of an access takes more cycles than a normal memory access.

**Spectre Attack using StealthyStreamline:** We demonstrate Spectre V1 attack [35] with the StealthyStreamline as the covert channel. Compared with the LRU address-based covert channel, the 2-bit StealthyStreamline enables us to encode 4x more symbols with the same cache. Compared with flush+reload or evict+time, StealthyStreamline makes the attack stealthier.

## VI. DISCUSSION AND FUTURE WORK

### A. Comparison with Search Algorithms

RL takes a fewer number of steps to find a successful attack than a brute-force search, and has the potential to handle much larger search spaces. Consider the prime+probe attack on an  $N$ -way cache set as an example. On average, we can find one prime+probe sequence every  $M$  sequences, where  $M = \frac{2 \times (N+1)^{2N+1}}{(N!)^2}$ . Since  $N! \sim \sqrt{2\pi N} \left(\frac{N}{e}\right)^{2N}$ , we have  $M \sim e^{2N}$ , which increases exponentially with the number of ways. For  $N = 8$ ,  $M \approx 2.05 \times 10^7$ , it takes about 369 million steps to find an attack, considering each attack sequence takes  $2N + 2$  steps. Last-level caches usually have more than 8 ways and it will be infeasible for exhaustive search. With RL, the agent converges within  $\sim 1$  million steps.

Compared to RL that learns policy/value on the fly to progressively improve the search quality to find the distinguishing sequence, traditional search techniques may not have sufficient learning capability. For example, a random search does not have learning at all; A\* search utilizes a predefined heuristics function, which was not updated during the search process.

### B. Cache with Randomized Mapping

To thwart set-based cache timing attacks, recent studies [59], [60], [66], [81] proposed changing the cache mapping and make it hard for the attacker to co-locate with the victim on desired cache sets. As a preliminary study, we implemented a randomized mapping scheme similar to CEASE [59], and tested AutoCAT with randomized mapping. Similar to CaSA [8], we assume an attacker can keep monitoring and learning the cache set mapping and launch an attack when needed. We use a 4-set 2-way cache in this experiment. The victim accesses address 0 or not depends on the secret. The attacker’s address range is 1-11. When randomizing the mapping, address 0-11 are randomly permuted and map to different sets. In Figure 7, we show the accuracy of the agent as the function of the training epochs. We set the redo the randomization 2M memory accesses. We found

that the attack accuracy drops after a randomized mapping, but the agent can adapt to the new mapping quickly within around 50 epochs in many cases.

It is also interesting to note that our preliminary result shows that the attack accuracy improves gradually even when an attacker does not have a full eviction set, which is the same observation made by the previous study [8] (there is a trade-off between calibration time and attack accuracy).

### C. Future Extensions

One challenge in AutoCAT lies in analyzing many attack sequences from the RL agent. We had to manually analyse and categorize the sequences found by AutoCAT. Ideally, we need to automated attack analysis.

Given the repetitive structure of a cache, we focus on training AutoCAT with small cache configurations and generalize the attack to real machines manually. The scalability and generalizability when applying to multiple levels of large caches still need to be further explored. Our initial investigation shows promising results that suggest AutoCAT can be further improved with new ML model architectures such as Transformers [13], [30], [78] and RL generalization methods [34], [61]. In the future work, we plan to investigate extending the AutoCAT approach to more complex cache configurations and other types of microarchitectural timing channels beyond cache.

We have demonstrated RL can find attacks wieht randomized mapping, however, it remains future work how quickly RL can adapt to dynamic remapping [59].

For training on real hardware, the CacheQuery interface only supports access on one cache set, which exclude possible attack sequences that involve multiple cache sets. We plan to make CacheQuery support measurement on multiple cache sets.

## VII. RELATED WORK

**Automated timing channel analysis and discovery.** Prior studies proposed systematic analysis methods for cache timing channels based on simplified cache models [17], [26], [84]. Our work demonstrates RL as a new way to enable more automated security analysis, which can be easily extended to new systems or defense mechanisms with less human effort. There exist other automated approaches for vulnerability analysis such as exhaustive approach [19], taint analysis [21], fuzzing [20], [48], [82], relational testing [52], and formal methods [75]. CheckMate [75] can only discover attacks that is specified by the given exploit sequence. Information flow tracking technique such as SecVerilog [94] can identify information leakage in the designs but cannot generate exploits automatically. For example, the attack sequences that exploit dirty bits [16] are only reported seven years after the vulnerability is noted by SecVerilog. Compared to formal methods, the RL-based method cannot provide mathematical security guarantees, but can more easily be applied to a system without building a formal model or writing proofs, both of which require significant human efforts [11]. Compared to fuzzing, the RL-based method is more efficient and expressive for complex attack sequences.

For example, Osiris [82] explores attack with three instructions, and IntroSpectre [20] relies on predefined attack gadgets.

**Cache-timing attack detection and defense.** To prevent cache timing-channel attacks, many detection and defense mechanisms were proposed. Detection mechanisms such as cc-Hunter [12] and ReplayConfusion [88] focus on detecting an attack. We show that the RL agent has the potential to automatically generate attacks to evade detection schemes. On the other hand, defenses [18], [33], [51], [60], [66], [74], [87] focus on mitigating or removing the interference that leads to known timing channels. This paper shows that RL also has the potential to automatically evaluate the security of mitigations, and shows that AutoCAT can break PLCache [81] successfully.

**ML for security.** Machine learning was used in the computer security domain for anomaly detection [38], website fingerprinting [37], [68], and other analysis tasks. However, traditional supervised learning cannot find new attacks without known attack sequences or labels. To address this challenge, we propose to use RL, which can be trained with delayed rewards and whose action trajectories are expressive enough to represent real-world attack sequences.

Reinforcement learning has been used for software security [50], IoT security [76], autonomous driving security [63], power side-channel attacks [62], circuit test generation [55], power side-channel countermeasures [64], and hardware Trojan detection [54]. To our knowledge, our work is the first of its kind in using RL to actively and automatically generate attack sequences in the microarchitecture security domain.

## VIII. CONCLUSION

In this paper, we propose to use reinforcement learning to automatically find existing and undiscovered timing-channel attack sequences. As a concrete example, we build the AutoCAT framework, which can explore cache-timing attacks in various cache configurations and attacker/victim settings, and under different defense and detection mechanisms. Our experimental results show that the RL agent can find practical attack sequences for various blackbox cache designs. The RL agent also discovered the StealthyStreamline attack, which is a novel attack with a higher bit-rate on real machines than attacks reported in previous literature. AutoCAT shows RL is a promising method to explore microarchitecture timing attacks in practical systems.

## ACKNOWLEDGMENT

The authors would like to thank John Ghra at Virginia Tech for technical support. Mulong Luo is partially supported by NSF under grant ECCS-1932501.

## REFERENCES

- [1] [Online]. Available: <https://github.com/auxiliary/CacheSimulator>
- [2] [Online]. Available: <https://openai.com/blog/openai-baselines-ppo>
- [3] A. Abel and J. Reineke, "Reverse engineering of cache replacement policies in intel microprocessors and their evaluation," in *2014 IEEE International Symposium on Performance Analysis of Systems and Software (ISPASS)*. IEEE, 2014, pp. 141–142.
- [4] M. Alam, S. Bhattacharya, D. Mukhopadhyay, and S. Bhattacharya, "Performance counters to rescue: A machine learning based safeguard against micro-architectural side-channel-attacks," *Cryptology ePrint Archive*, 2017.
- [5] S. Berner, G. Brockman, B. Chan, V. Cheung, P. Debiak, C. Dennison, D. Farhi, Q. Fischer, S. Hashme, C. Hesse *et al.*, "Dota 2 with large scale deep reinforcement learning," *arXiv preprint arXiv:1912.06680*, 2019.
- [6] D. J. Bernstein, "Cache-timing attacks on AES."
- [7] J. Bonneau and I. Mironov, "Cache-collision timing attacks against aes," in *International Workshop on Cryptographic Hardware and Embedded Systems*. Springer, 2006, pp. 201–215.
- [8] T. Bourgeat, J. Drean, Y. Yang, L. Tsai, J. Emer, and M. Yan, "CaSA: End-to-end quantitative security analysis of randomly mapped caches," in *2020 53rd Annual IEEE/ACM International Symposium on Microarchitecture (MICRO)*. IEEE, 2020, pp. 1110–1123.
- [9] S. Briongos, P. Malagón, J. M. Moya, and T. Eisenbarth, "RELOAD+REFRESH: Abusing cache replacement policies to perform stealthy cache attacks," in *29th USENIX Security Symposium (USENIX Security 20)*, 2020, pp. 1967–1984.
- [10] G. Brockman, V. Cheung, L. Pettersson, J. Schneider, J. Schulman, J. Tang, and W. Zaremba, "Openai gym," 2016.
- [11] P. Buiras, H. Nemati, A. Lindner, and R. Guanciale, "Validation of side-channel models via observation refinement," in *MICRO-54: 54th Annual IEEE/ACM International Symposium on Microarchitecture*, 2021, pp. 578–591.
- [12] J. Chen and G. Venkataramani, "CC-hunter: Uncovering covert timing channels on shared processor hardware," in *2014 47th Annual IEEE/ACM International Symposium on Microarchitecture*. IEEE, 2014, pp. 216–228.
- [13] L. Chen, K. Lu, A. Rajeswaran, K. Lee, A. Grover, M. Laskin, P. Abbeel, A. Srinivas, and I. Mordatch, "Decision transformer: Reinforcement learning via sequence modeling," in *Advances in Neural Information Processing Systems*, A. Beygelzimer, Y. Dauphin, P. Liang, and J. W. Vaughan, Eds., 2021. [Online]. Available: <https://openreview.net/forum?id=a7APmM4B9d>
- [14] Y. Chen, L. Pei, and T. E. Carlson, "Leaking control flow information via the hardware prefetcher," *arXiv preprint arXiv:2109.00474*, 2021.
- [15] M. Chiappetta, E. Savas, and C. Yilmaz, "Real time detection of cache-based side-channel attacks using hardware performance counters," *Applied Soft Computing*, vol. 49, pp. 1162–1174, 2016.
- [16] Y. Cui and X. Cheng, "Abusing cache line dirty states to leak information in commercial processors," in *2022 IEEE International Symposium on High Performance Computer Architecture (HPCA)*. IEEE, 2022.
- [17] S. Deng, W. Xiong, and J. Szefer, "A benchmark suite for evaluating caches' vulnerability to timing attacks," in *Proceedings of the Twenty-Fifth International Conference on Architectural Support for Programming Languages and Operating Systems*, 2020, pp. 683–697.
- [18] G. Dessouky, T. Frassetto, and A.-R. Sadeghi, "HybCache: Hybrid side-channel-resilient caches for trusted execution environments," in *29th USENIX Security Symposium (USENIX Security 20)*, 2020, pp. 451–468.
- [19] M. R. Fadiheh, A. Wezel, J. Muller, J. Bormann, S. Ray, J. M. Fung, S. Mitra, D. Stoffel, and W. Kunz, "An exhaustive approach to detecting transient execution side channels in RTL designs of processors," *IEEE Transactions on Computers*, 2022.
- [20] M. Ghaniyoun, K. Barber, Y. Zhang, and R. Teodorescu, "IntroSpectre: a pre-silicon framework for discovery and analysis of transient execution vulnerabilities," in *2021 ACM/IEEE 48th Annual International Symposium on Computer Architecture (ISCA)*. IEEE, 2021, pp. 874–887.
- [21] B. Gras, C. Giuffrida, M. Kurth, H. Bos, and K. Razavi, "ABSynthe: Automatic blackbox side-channel synthesis on commodity microarchitectures," in *Network and Distributed Systems Security (NDSS) Symposium*, 2020.
- [22] D. Gruss, C. Maurice, K. Wagner, and S. Mangard, "Flush+ Flush: a fast and stealthy cache attack," in *International Conference on Detection of Intrusions and Malware, and Vulnerability Assessment*. Springer, 2016, pp. 279–299.
- [23] J. Hare, "Dealing with sparse rewards in reinforcement learning," *arXiv preprint arXiv:1910.09281*, 2019.
- [24] A. Harris, S. Wei, P. Sahu, P. Kumar, T. Austin, and M. Tiwari, "Cyclone: Detecting contention-based cache information leaks through cyclic interference," in *Proceedings of the 52nd Annual IEEE/ACM International Symposium on Microarchitecture*, 2019, pp. 57–72.

- [25] T. Hastie, R. Tibshirani, J. H. Friedman, and J. H. Friedman, *The elements of statistical learning: data mining, inference, and prediction*. Springer, 2009, vol. 2.
- [26] Z. He and R. B. Lee, "How secure is your cache against side-channel attacks?" in *Proceedings of the 50th Annual IEEE/ACM International Symposium on Microarchitecture*, 2017, pp. 341–353.
- [27] S. Hochreiter and J. Schmidhuber, "Long Short-Term Memory," *Neural Comput.*, vol. 9, no. 8, Nov. 1997.
- [28] Y. Hsiao, D. P. Mulligan, N. Nikoleris, G. Petri, and C. Trippel, "Synthesizing formal models of hardware from rtl for efficient verification of memory model implementations," in *MICRO-54: 54th Annual IEEE/ACM International Symposium on Microarchitecture*, 2021, pp. 679–694.
- [29] A. Jaleel, K. B. Theobald, S. C. Steely Jr, and J. Emer, "High performance cache replacement using re-reference interval prediction (RRIP)," *ACM SIGARCH Computer Architecture News*, vol. 38, no. 3, pp. 60–71, 2010.
- [30] M. Janner, Q. Li, and S. Levine, "Offline reinforcement learning as one big sequence modeling problem," in *Advances in Neural Information Processing Systems*, 2021.
- [31] N. P. Jouppi, "Improving direct-mapped cache performance by the addition of a small fully-associative cache and prefetch buffers," *ACM SIGARCH Computer Architecture News*, vol. 18, no. 2SI, pp. 364–373, 1990.
- [32] D. P. Kingma and J. Ba, "Adam: A method for stochastic optimization," in *ICLR (Poster)*, 2015. [Online]. Available: <http://arxiv.org/abs/1412.6980>
- [33] V. Kiriansky, I. Lebedev, S. Amarasinghe, S. Devadas, and J. Emer, "DAWG: A defense against cache timing attacks in speculative execution processors," in *2018 51st Annual IEEE/ACM International Symposium on Microarchitecture (MICRO)*. IEEE, 2018, pp. 974–987.
- [34] R. Kirk, A. Zhang, E. Grefenstette, and T. Rocktäschel, "A survey of generalisation in deep reinforcement learning," *CoRR*, vol. abs/2111.09794, 2021. [Online]. Available: <https://arxiv.org/abs/2111.09794>
- [35] P. Kocher, J. Horn, A. Fogh, D. Genkin, D. Gruss, W. Haas, M. Hamburg, M. Lipp, S. Mangard, T. Prescher *et al.*, "Spectre attacks: Exploiting speculative execution," in *2019 IEEE Symposium on Security and Privacy (SP)*. IEEE, 2019, pp. 1–19.
- [36] Y. Kulah, B. Dincer, C. Yilmaz, and E. Savas, "SpyDetector: An approach for detecting side-channel attacks at runtime," *International Journal of Information Security*, vol. 18, no. 4, pp. 393–422, 2019.
- [37] A. S. La Cour, K. K. Afridi, and G. E. Suh, "Wireless charging power side-channel attacks," in *Proceedings of the 2021 ACM SIGSAC Conference on Computer and Communications Security*, 2021, pp. 651–665.
- [38] T. D. Lane, *Machine learning techniques for the computer security domain of anomaly detection*. Purdue University, 2000.
- [39] A. Lazaric, "Transfer in reinforcement learning: a framework and a survey," in *Reinforcement Learning*. Springer, 2012, pp. 143–173.
- [40] E. Liang, R. Liaw, R. Nishihara, P. Moritz, R. Fox, K. Goldberg, J. Gonzalez, M. Jordan, and I. Stoica, "RLlib: Abstractions for distributed reinforcement learning," in *International Conference on Machine Learning*. PMLR, 2018, pp. 3053–3062.
- [41] M. Lipp, D. Gruss, R. Spreitzer, C. Maurice, and S. Mangard, "AR-Mageddon: Cache attacks on mobile devices," in *25th USENIX Security Symposium (USENIX Security 16)*, 2016, pp. 549–564.
- [42] M. Lipp, M. Schwarz, D. Gruss, T. Prescher, W. Haas, A. Fogh, J. Horn, S. Mangard, P. Kocher, D. Genkin *et al.*, "Meltdown: Reading kernel memory from user space," in *27th USENIX Security Symposium (USENIX Security 18)*, 2018, pp. 973–990.
- [43] F. Liu, Y. Yarom, Q. Ge, G. Heiser, and R. B. Lee, "Last-level cache side-channel attacks are practical," in *2015 IEEE symposium on security and privacy*. IEEE, 2015, pp. 605–622.
- [44] M. Luo, A. C. Myers, and G. E. Suh, "Stealthy tracking of autonomous vehicles with cache side channels," in *29th USENIX Security Symposium (USENIX Security 20)*. USENIX Association, Aug. 2020, pp. 859–876.
- [45] Y. Michalevsky, A. Schulman, G. A. Veerapandian, D. Boneh, and G. Nakibly, "PowerSpy: Location tracking using mobile device power analysis," in *24th USENIX Security Symposium (USENIX Security 15)*, 2015, pp. 785–800.
- [46] S. Mirbagher-Ajorpaz, G. Pokam, E. Mohammadian-Koruyeh, E. Garza, N. Abu-Ghazaleh, and D. A. Jiménez, "Perspectron: Detecting invariant footprints of microarchitectural attacks with perceptron," in *2020 53rd Annual IEEE/ACM International Symposium on Microarchitecture (MICRO)*. IEEE, 2020, pp. 1124–1137.
- [47] V. Mnih, K. Kavukcuoglu, D. Silver, A. A. Rusu, J. Veness, M. G. Bellemare, A. Graves, M. Riedmiller, A. K. Fidjeland, G. Ostrovski, S. Petersen, C. Beattie, A. Sadik, I. Antonoglou, H. King, D. Kumaran, D. Wierstra, S. Legg, and D. Hassabis, "Human-level control through deep reinforcement learning," *Nature*, vol. 518, no. 7540, pp. 529–533, Feb. 2015, publisher: Nature Publishing Group, a division of Macmillan Publishers Limited. All Rights Reserved.
- [48] D. Moghimi, M. Lipp, B. Sunar, and M. Schwarz, "Medusa: Microarchitectural data leakage via automated attack synthesis," in *29th USENIX Security Symposium (USENIX Security 20)*, 2020, pp. 1427–1444.
- [49] S. Narvekar, B. Peng, M. Leonetti, J. Sinapov, M. E. Taylor, and P. Stone, "Curriculum learning for reinforcement learning domains: A framework and survey," *arXiv preprint arXiv:2003.04960*, 2020.
- [50] T. T. Nguyen and V. J. Reddi, "Deep reinforcement learning for cyber security," *IEEE Transactions on Neural Networks and Learning Systems*, 2019.
- [51] D. Ojha and S. Dwarkadas, "TimeCache: using time to eliminate cache side channels when sharing software," in *2021 ACM/IEEE 48th Annual International Symposium on Computer Architecture (ISCA)*. IEEE, 2021, pp. 375–387.
- [52] O. Oleksenko, C. Fetzer, B. Köpf, and M. Silberstein, "Revizor: testing black-box cpus against speculation contracts," in *Proceedings of the 27th ACM International Conference on Architectural Support for Programming Languages and Operating Systems*, 2022, pp. 226–239.
- [53] D. A. Osvik, A. Shamir, and E. Tromer, "Cache attacks and countermeasures: the case of AES," in *Cryptographers' track at the RSA conference*. Springer, 2006, pp. 1–20.
- [54] Z. Pan and P. Mishra, "Automated test generation for hardware trojan detection using reinforcement learning." New York, NY, USA: Association for Computing Machinery, 2021.
- [55] Z. Pan, J. Sheldon, and P. Mishra, "Test generation using reinforcement learning for delay-based side-channel analysis," in *2020 IEEE/ACM International Conference On Computer Aided Design (ICCAD)*. IEEE, 2020, pp. 1–7.
- [56] A. Paszke, S. Gross, F. Massa, A. Lerer, J. Bradbury, G. Chanan, T. Killeen, Z. Lin, N. Gimelshein, L. Antiga, A. Desmaison, A. Kopf, E. Yang, Z. DeVito, M. Raison, A. Tejani, S. Chilamkurthy, B. Steiner, L. Fang, J. Bai, and S. Chintala, "PyTorch: An imperative style, high-performance deep learning library," in *Advances in Neural Information Processing Systems 32*, H. Wallach, H. Larochelle, A. Beygelzimer, F. d'Alché-Buc, E. Fox, and R. Garnett, Eds. Curran Associates, Inc., 2019, pp. 8024–8035. [Online]. Available: <http://papers.neurips.cc/paper/9015-pytorch-an-imperative-style-high-performance-deep-learning-library.pdf>
- [57] W. Perez, E. Sanchez, M. S. Reorda, A. Tonda, and J. V. Medina, "Functional test generation for the plru replacement mechanism of embedded cache memories," in *2011 12th Latin American Test Workshop (LATW)*. IEEE, 2011, pp. 1–6.
- [58] M. L. Puterman, "Markov decision processes: Discrete stochastic dynamic programming," *Journal of the Operational Research Society*, 1995.
- [59] M. K. Qureshi, "Ceaser: Mitigating conflict-based cache attacks via encrypted-address and remapping," in *2018 51st Annual IEEE/ACM International Symposium on Microarchitecture (MICRO)*. IEEE, 2018, pp. 775–787.
- [60] M. K. Qureshi, "New attacks and defense for encrypted-address cache," in *2019 ACM/IEEE 46th Annual International Symposium on Computer Architecture (ISCA)*. IEEE, 2019, pp. 360–371.
- [61] R. Raileanu, M. Goldstein, D. Yarats, I. Kostrikov, and R. Fergus, "Automatic Data Augmentation for Generalization in Reinforcement Learning," in *Advances in Neural Information Processing Systems*, M. Ranzato, A. Beygelzimer, Y. Dauphin, P. S. Liang, and J. W. Vaughan, Eds., vol. 34. Curran Associates, Inc., 2021, pp. 5402–5415. [Online]. Available: <https://proceedings.neurips.cc/paper/2021/file/2b38c2df6a49b97f706ec9148ce48d86-Paper.pdf>
- [62] K. Ramezanpour, P. Ampadu, and W. Diehl, "SCARL: side-channel analysis with reinforcement learning on the ascon authenticated cipher," *arXiv preprint arXiv:2006.03995*, 2020.
- [63] I. Rasheed, F. Hu, and L. Zhang, "Deep reinforcement learning approach for autonomous vehicle systems for maintaining security and safety using LSTM-GAN," *Vehicular Communications*, vol. 26, p. 100266, 2020.
- [64] J. Rijdsdijk, L. Wu, and G. Perin, "Reinforcement learning-based design of side-channel countermeasures," *Cryptology ePrint Archive*, Report 2021/526, 2021, <https://ia.cr/2021/526>.
- [65] G. Saileshwar, C. W. Fletcher, and M. Qureshi, "Streamline: a fast, flush-less cache covert-channel attack by enabling asynchronous collusion," in *Proceedings of the 26th ACM International Conference on Architectural*

*Support for Programming Languages and Operating Systems*, 2021, pp. 1077–1090.

- [66] G. Saileshwar and M. Qureshi, “MIRAGE: Mitigating conflict-based cache attacks with a practical fully-associative design,” in *30th USENIX Security Symposium (USENIX Security 21)*, 2021, pp. 1379–1396.
- [67] J. Schulman, F. Wolski, P. Dhariwal, A. Radford, and O. Klimov, “Proximal policy optimization algorithms,” *arXiv preprint arXiv:1707.06347*, 2017.
- [68] A. Shusterman, L. Kang, Y. Haskal, Y. Meltser, P. Mittal, Y. Oren, and Y. Yarom, “Robust website fingerprinting through the cache occupancy channel,” in *28th USENIX Security Symposium (USENIX Security 19)*, 2019, pp. 639–656.
- [69] D. Silver, A. Huang, C. J. Maddison, A. Guez, L. Sifre, G. van den Driessche, J. Schrittwieser, I. Antonoglou, V. Panneershelvam, M. Lanctot, S. Dieleman, D. Grewe, J. Nham, N. Kalchbrenner, I. Sutskever, T. Lillicrap, M. Leach, K. Kavukcuoglu, T. Graepel, and D. Hassabis, “Mastering the Game of Go with Deep Neural Networks and Tree Search,” *Nature*, vol. 529, no. 7587, pp. 484–489, Jan. 2016.
- [70] D. Silver, J. Schrittwieser, K. Simonyan, I. Antonoglou, A. Huang, A. Guez, T. Hubert, L. Baker, M. Lai, A. Bolton *et al.*, “Mastering the game of go without human knowledge,” *nature*, vol. 550, no. 7676, pp. 354–359, 2017.
- [71] A. J. Smith, “Cache memories,” *ACM Computing Surveys (CSUR)*, vol. 14, no. 3, pp. 473–530, 1982.
- [72] K. So and R. N. Rechtschaffen, “Cache operations by mru change,” *IEEE Transactions on Computers*, vol. 37, no. 6, pp. 700–709, 1988.
- [73] R. S. Sutton and A. G. Barto, *Reinforcement learning: An introduction*, 2nd ed. MIT press, 2018.
- [74] Q. Tan, Z. Zeng, K. Bu, and K. Ren, “PhantomCache: Obfuscating cache conflicts with localized randomization,” in *Networked and Distributed System Symposium (NDSS)*, 2020.
- [75] C. Trippel, D. Lustig, and M. Martonosi, “CheckMate: Automated synthesis of hardware exploits and security litmus tests,” in *2018 51st Annual IEEE/ACM International Symposium on Microarchitecture (MICRO)*. IEEE, 2018, pp. 947–960.
- [76] A. Uprety and D. B. Rawat, “Reinforcement learning for iot security: A comprehensive survey,” *IEEE Internet of Things Journal*, vol. 8, no. 11, pp. 8693–8706, 2020.
- [77] A. Vaswani, N. Shazeer, N. Parmar, J. Uszkoreit, L. Jones, A. N. Gomez, L. Kaiser, and I. Polosukhin, “Attention is all you need,” *Advances in neural information processing systems*, vol. 30, 2017.
- [78] A. Vaswani, N. Shazeer, N. Parmar, J. Uszkoreit, L. Jones, A. N. Gomez, L. Kaiser, and I. Polosukhin, “Attention is All you Need,” in *Advances in Neural Information Processing Systems*, I. Guyon, U. V. Luxburg, S. Bengio, H. Wallach, R. Fergus, S. Vishwanathan, and R. Garnett, Eds., vol. 30. Curran Associates, Inc., 2017. [Online]. Available: <https://proceedings.neurips.cc/paper/2017/file/3f5ee243547dee91fbd053c1c4a845aa-Paper.pdf>
- [79] P. Vila, P. Ganty, M. Guarnieri, and B. Köpf, “CacheQuery: Learning replacement policies from hardware caches,” in *Proceedings of the 41st ACM SIGPLAN Conference on Programming Language Design and Implementation*, 2020, pp. 519–532.
- [80] D. Wang, Z. Qian, N. Abu-Ghazaleh, and S. V. Krishnamurthy, “Papp: Prefetcher-aware prime and probe side-channel attack,” in *Proceedings of the 56th Annual Design Automation Conference 2019*, 2019, pp. 1–6.
- [81] Z. Wang and R. B. Lee, “New cache designs for thwarting software cache-based side channel attacks,” in *Proceedings of the 34th annual international symposium on Computer architecture*, 2007, pp. 494–505.
- [82] D. Weber, A. Ibrahim, H. Nemati, M. Schwarz, and C. Rossow, “Osiris: Automated discovery of microarchitectural side channels,” in *30th USENIX Security Symposium (USENIX Security 21)*, 2021, pp. 1415–1432.
- [83] L. Wei, B. Luo, Y. Li, Y. Liu, and Q. Xu, “I know what you see: Power side-channel attack on convolutional neural network accelerators,” in *Proceedings of the 34th Annual Computer Security Applications Conference*, 2018, pp. 393–406.
- [84] Y. Xiao, Y. Zhang, and R. Teodorescu, “SPEECHMINER: A framework for investigating and measuring speculative execution vulnerabilities,” *arXiv preprint arXiv:1912.00329*, 2019.
- [85] W. Xiong, S. Katzenbeisser, and J. Szefer, “Leaking information through cache LRU states in commercial processors and secure caches,” *IEEE Transactions on Computers*, vol. 70, no. 4, pp. 511–523, 2021.
- [86] W. Xiong and J. Szefer, “Leaking information through cache LRU states,” in *2020 IEEE International Symposium on High Performance Computer Architecture (HPCA)*. IEEE, 2020, pp. 139–152.
- [87] M. Yan, B. Gopireddy, T. Shull, and J. Torrellas, “Secure hierarchy-aware cache replacement policy (SHARP): Defending against cache-based side channel attacks,” in *2017 ACM/IEEE 44th Annual International Symposium on Computer Architecture (ISCA)*. IEEE, 2017, pp. 347–360.
- [88] M. Yan, Y. Shalabi, and J. Torrellas, “ReplayConfusion: detecting cache-based covert channel attacks using record and replay,” in *2016 49th Annual IEEE/ACM International Symposium on Microarchitecture (MICRO)*. IEEE, 2016, pp. 1–14.
- [89] M. Yan, R. Sprabery, B. Gopireddy, C. Fletcher, R. Campbell, and J. Torrellas, “Attack directories, not caches: Side channel attacks in a non-inclusive world,” in *2019 IEEE Symposium on Security and Privacy (SP)*. IEEE, 2019, pp. 888–904.
- [90] X. Yang, B. Cui, T. Li, and Y. Tian, “RLMeta: A Flexible Framework for Distributed Reinforcement Learning,” 1 2022. [Online]. Available: <https://github.com/facebookresearch/rlmeta>
- [91] F. Yao, M. Doroslovacki, and G. Venkataramani, “Are coherence protocol states vulnerable to information leakage?” in *2018 IEEE International Symposium on High Performance Computer Architecture (HPCA)*. IEEE, 2018, pp. 168–179.
- [92] Y. Yarom and K. Falkner, “FLUSH+ RELOAD: A high resolution, low noise, 13 cache side-channel attack,” in *23rd USENIX security symposium (USENIX security 14)*, 2014, pp. 719–732.
- [93] Y. Yuan, Q. Pang, and S. Wang, “Automated side channel analysis of media software with manifold learning,” in *31st USENIX Security Symposium (USENIX Security 22)*. Boston, MA: USENIX Association, Aug. 2022. [Online]. Available: <https://www.usenix.org/conference/usenixsecurity22/presentation/yuan-yuanyuan>
- [94] D. Zhang, Y. Wang, G. E. Suh, and A. C. Myers, “A hardware design language for timing-sensitive information-flow security,” *ASPLOS '15*, p. 503–516, 2015. [Online]. Available: <https://doi.org/10.1145/2694344.2694372>
- [95] T. Zhang, Y. Zhang, and R. B. Lee, “CloudRadar: A real-time side-channel attack detection system in clouds,” in *International Symposium on Research in Attacks, Intrusions, and Defenses*. Springer, 2016, pp. 118–140.

## APPENDIX

### A. Stability of Training and Impact of Reward Values

In AutoCAT, the agent gets a huge positive or negative reward when making a guess depending on the correctness, while getting constant reward otherwise. This is a type of *sparse reward*. Reinforcement Learning algorithms can wander aimlessly or stuck at local optima when dealing with sparse reward [23], [73]. The learning speed and accuracy of RL also have some correlation to reward values, especially for simple MLP models. Reward values using domain knowledge can improve the performance of an RL agent. As our goal is to train an agent that can guess the secret ( $\text{addr}_{\text{secret}}$ ) correctly with minimal number of steps, we chose a positive value for `correct_reward`, negative values for `wrong_reward` and `step_reward`.

We evaluated the impact of reward values on the performance of the RL agent by changing the reward values using the default three-layer MLP model. When the agent reaches 95% accuracy, we consider an attack pattern is found. We chose three metrics to evaluate the agent: 1) the number of time steps in  $10^3$  until convergence, 2) clock time in hours until convergence, and 3) episode lengths when the attack is found, i.e., the length of the attack. For each metric, the results of average (minimum, maximum) values are presented to show the variation between the training trials in Tables XI, Table XII, and Table XIII. As a baseline, we use the reward values of `correct_reward =`

200, `wrong_reward` = -10,000, and `step_reward` = -10. We evaluated an 8-way cache set. The victim either accesses cache line 0 or makes no access. The attacker address range is 1 to 8. Each configuration has been tested for 3 random seeds. **Scale of rewards.** In Table XI, we keep the ratio of the reward values but change the scale of the rewards. The result suggests that the learning performance is relatively stable even though the absolute values of the rewards do impact the performance. This is because we use Adam optimizer in which the step formula is invariant to diagonal rescaling of the gradients [32]. **Wrong-guess reward.** We test how training is affected by the wrong-guess reward values. As shown in Table XII, the agent converges slightly faster than the baseline when the penalty is larger. There is no significant difference in episode length. When `correct_reward` = 200 and `wrong_reward` is -1,000, the agent sometimes fails to find an attack and converges to a random guess.

**Step reward.** In Table XIII, we show the results when the step reward changes. Learning speed is improved by decreasing the step from -50 to 0. This is because the step penalty discourages the RL agent from exploring longer attack patterns which could lead to a successful attack. However, a larger step penalty results in a shorter attack pattern.

We also found that the Transformer model is less sensitive to the reward value settings. For our experiments with a Transformer model, we used the reward of `correct_reward` = 1, `wrong_reward` = -1, and `step_reward` = -0.01.

### B. Cache Guessing Game as Markov Decision Process

In this section, we discuss how a cache guessing game can be formulated as a Markov Decision Process (MDP). In general, the goal of an RL agent is to maximize the long-term rewards by finding a policy that generates a proper action sequence in a Markov Decision Process (MDP [58]). More specifically, the MDP is specified by the tuple  $\mathcal{M} = (\mathcal{S}, \mathcal{A}, \mathcal{P}, \mathcal{R}, \gamma)$ , where  $\mathcal{S}$  is the state space,  $\mathcal{A}$  the action space,  $\mathcal{P}(s'|s, a)$  the probability of transitioning from state  $s \in \mathcal{S}$  to state  $s' \in \mathcal{S}$ , and  $\gamma \in [0, 1)$  a discount factor. The state and action spaces can be either discrete or continuous. An “agent” chooses actions  $a \in \mathcal{A}$  according to a policy function  $a \sim \pi(s)$ , which updates the system state  $s' \sim \mathcal{P}(s, a)$ , yielding a reward  $r = \mathcal{R}(s) \in \mathbb{R}$ . The goal of the agent is to learn an optimal policy

TABLE XI: Training with different reward scales.

Metrics	Magnitude of reward scale		
	0.01x	0.1x	1x
attack found?	●	●	●
steps ( $10^3$ )	861 (696, 1080)	681 (552, 884)	889 (816, 1000)
time (h)	4.4 (3.6, 5.5)	3.6 (3.0, 4.8)	4.5 (4.3, 5.0)
episode length	30.27 (28.60, 32.98)	26.34 (23.02, 29.54)	29.53 (14.97, 37.24)

TABLE XII: Training with different wrong-guess rewards.

Metrics	Wrong guess reward		
	-1,000	-10,000	-100,000
attack found?	●	●	●
steps ( $10^3$ )	1038 (1000, 1076)	889 (816, 1000)	852 (780, 992)
time (h)	5.1 (4.8, 5.4)	4.5 (4.3, 5.0)	3.4 (2.3, 4.6)
episode length	25.04 (22.27, 27.81)	29.53 (14.97, 37.24)	30.74 (27.40, 35.00)

TABLE XIII: Training with different step rewards.

Metrics	Step reward				
	0	-2	-10	-25	-50
attack found?	●	●	●	●	●
steps ( $10^3$ )	713 (672, 788)	833 (648, 988)	889 (816, 1000)	1004 (808, 1284)	1977 (464, 3712)
time (h)	2.2 (2.0, 2.5)	3.8 (2.6, 5.3)	4.5 (4.3, 5.0)	4.0 (3.3, 5.3)	7.7 (1.9, 13.8)
episode length	25.94 (23.00, 29.58)	25.23 (16.39, 29.86)	29.53 (14.97, 37.24)	28.29 (19.28, 32.80)	21.62 (13.16, 25.85)

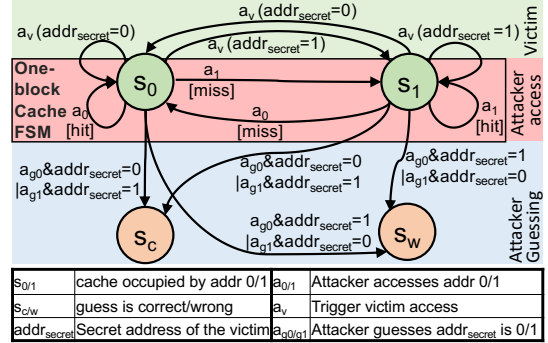


Fig. 8: MDP formulation of cache guessing game for an example one-block cache with only two cache lines. [hit/miss] indicates the observation during a transition.

$(\max_{\pi} \mathbb{E}_{\mathcal{P}} [\sum_{t=0}^{\infty} \gamma^t \mathcal{R}(s_t)])$  that takes in states and outputs actions to maximize the cumulative reward over some horizon. As cache-timing attacks exploit the internal states of a cache, the cache guessing game can be seen as an MDP that optimizes the correct guessing rate. In our cache guessing game, the long-term reward is defined as whether the victim’s information has been retrieved within a fixed number of steps.

To show the theoretical foundation, here we consider a toy cache example with only one cache block and two cache lines 0 and 1. This simple cache can be represented by a tuple  $\mathcal{M} = (\mathcal{S}, \mathcal{A}, \mathcal{P})$  where  $\mathcal{S} = \{s_0, s_1\}$  contains the all cache states representing which addr (0 or 1) is in the cache,  $\mathcal{A} = \{a_0, a_1\}$  contains actions that access address 0/1, and  $\mathcal{P}$  has the transition rules, shown as the arrows in Figure 8.

We can formulate the cache guessing game based on the the of the cache with the additional state transitions for the victim’s accesses ( $a_v$ ) and the attacker’s guess ( $a_{g0}$  or  $a_{g1}$ ). In a typical cache timing-channel threat model, the victim holds a secret address  $addr_{secret}$  which is unknown to the attacker. For example, if the secret address is either address 0 or address 1, then we can add an action  $a_v$  to  $\mathcal{A}$  to represent an access to the secret address. As the attacker does not know the secret address, this action may lead to  $s_0$  or  $s_1$  depending on the secret as shown in Figure 8. We add two actions  $a_{g0}$  and  $a_{g1}$  to  $\mathcal{A}$  indicating that the attacker makes a guess that the secret address is 0 or 1. We also add two additional states  $s_c$  and  $s_w$  to  $\mathcal{S}$  to represent the guess is correct or wrong. The transition  $\mathcal{P}$  depends on  $addr_{secret}$ .

A successful attack sequence that can be represented as a path starting from  $s_0$  or  $s_1$  and ends in  $s_c$  in Figure 8, whereas a failed attack sequence ends in  $s_w$ . The goal is to find as many successful attacks as possible. For example, assume we start

with  $s_0$ , and we want to end in  $s_c$ . We can reach  $s_c$  by taking action  $a_{g0}$  or  $a_{g1}$  depending on the value of  $addr_{secret}$ , which is unknown to the attacker. However,  $addr_{secret}$  can be inferred by the state after  $a_v$ . For example, if after  $a_v$  it ends in  $s_1$ , then  $addr_{secret}$  must be 1. To infer the current state, we can do  $a_1$  and observe the hit/miss response. Thus, if  $addr_{secret} = 1$ , a successful attack sequence can be:  $s_0 \rightarrow a_v \rightarrow s_1 \rightarrow a_1(\text{hit}) \rightarrow s_1 \rightarrow a_{g1} \rightarrow s_c$ . Similarly, if  $addr_{secret} = 0$ , a successful attack sequence can be:  $s_0 \rightarrow a_v \rightarrow s_0 \rightarrow a_1(\text{miss}) \rightarrow s_1 \rightarrow a_{g0} \rightarrow s_c$ .

This example shows that for all possible values of  $addr_{secret}$  and initial states if we can enumerate all paths that lead to  $s_c$ , we can find all possible attacks. However, this search approach does not work in practice for the following reasons:

- 1) It is difficult to know the exact representations of the MDP because the detailed microarchitectural operations are often kept as proprietary confidential know how by chip designers. Reverse engineering effort can be onerous and only reveal limited information [3], [79].
- 2) The state is not fully visible to the attacker because the state depends on other processes' cache entries.
- 3) The MDP can be quite complex because of a replacement-state [57], cache directory [89], cache prefetcher [14], [80], etc. The composition of these FSMs multiplies the number of states and transitions, making optimization-based methods intractable.
- 4) Microarchitectural operations can be pseudo-random such as random replacement algorithms, meaning the transitions inside the MDP are not entirely predictable.

Due to these difficulties, directly using a search approach to enumerate all possible paths and find successful attacks is not practical. Instead, we use RL that does not need full observation of the state space. Applying RL to the cache-timing attack, we only need to define the rewards  $\mathcal{R}$  and a black box cache model.